applied sciences

MDPI

Article

Novel Graphical Representation and Numerical Characterization of DNA Sequences

Chun Li [1,2,*], Wenchao Fei [1], Yan Zhao [1] and Xiaoqing Yu [3]

[1] Department of Mathematics, Bohai University, Jinzhou 121013, China; feiwenchao90@163.com (W.F.); zhaoyan_jinzh@126.com (Y.Z.)

[2] Research Institute of Food Science, Bohai University, Jinzhou 121013, China

[3] Department of Applied Mathematics, Shanghai Institute of Technology, Shanghai 201418, China; xqyu@sit.edu.cn

* Correspondence: lichwun@163.com; Tel.: +86-416-3402166

Academic Editor: Yang Kuang
Received: 10 December 2015; Accepted: 14 February 2016; Published: 24 February 2016

Abstract: Modern sequencing technique has provided a wealth of data on DNA sequences, which has made the analysis and comparison of sequences a very important but difficult task. In this paper, by regarding the dinucleotide as a 2-combination of the multiset $\{\infty \cdot A, \infty \cdot G, \infty \cdot C, \infty \cdot T\}$, a novel 3-D graphical representation of a DNA sequence is proposed, and its projections on planes (x,y), (y,z) and (x,z) are also discussed. In addition, based on the idea of "piecewise function", a cell-based descriptor vector is constructed to numerically characterize the DNA sequence. The utility of our approach is illustrated by the examination of phylogenetic analysis on four datasets.

Keywords: 2-combination; graphical representation; cell-based vector; numerical characterization; phylogenetic analysis

1. Introduction

The rapid development of DNA sequencing techniques has resulted in explosive growth in the number of DNA primary sequences, and the analysis and comparison of biological sequences has become a topic of considerable interest in Computational Biology and Bioinformatics. The traditional measure for similarity analysis of DNA sequences is based on multiple sequence alignment, which uses dynamic programming techniques to identify the globally optimal alignment solution. However, the sequence alignment problem is NP-hard (non-deterministic polynomial-time hard), making it infeasible for dealing with large datasets [1]. To overcome the limitation, a lot of alignment-free approaches for sequence comparison have been proposed.

The basic idea behind most alignment-free methods is to characterize DNA by certain mathematical models derived for DNA sequence, rather than by a direct comparison of DNA sequences themselves. Graphical representation is deemed to be a simple and powerful tool for the visualization and analysis of bio-sequences. The earliest attempts at the graphical representation of DNA sequences were made by Hamori and Ruskin in 1983 [2]. Afterwards, a number of graphical representations were well developed by researchers. For instance, by assigning four directions defined by the positive/negative x and y coordinate axes to the four nucleic acid bases, Gates [3], Nandy [4,5], and Leong and Morgenthaler [6] introduced three different 2-D graphical representations, respectively. While Jeffrey [7] proposed a chaos game representation (CGR) of DNA sequences, in which the four corners of a selected square are associated with the four bases respectively. In 2000, Randic *et al.* [8] generalized these 2-D graphical representations to a 3-D graphical representation, in which the center of a cube is chosen as the origin of the Cartesian (x,y,z) coordinate system, and the four corners with coordinates (+1,−1,−1), (−1,+1,−1), (−1,−1,+1), and (+1,+1,+1) are assigned to the four bases. Some other graphical representations of bio-sequences and their applications in the field of biological science and technology can be found in [9–24].

Numerical characterization is another useful tool for sequence comparison. One way to arrive at the numerical characterization of a DNA sequence is to associate the sequence with a vector whose components are related to *k*-words, including the single nucleotide, dinucleotide, trinucleotide, and so on [25–30]. In addition, the numerical characterization can be accomplished by associating with a graphical representation given by a curve in the space (or a plane) structural matrices, such as the Euclidean-distance matrix (ED), the graph theoretical distance matrix (GD), the quotient matrix (D/D, M/M, L/L), and their "higher order" matrices [8–18,31–33]. Once a matrix representation of a DNA sequence is given, some matrix invariants, e.g. the leading eigenvalues, can be used as descriptors of the sequence. This technique has been widely used in the field of biological science and medicine, and different types of matrices are defined to construct various invariants of DNA sequences. However, the order of these matrices is equal to *n*, the length of the DNA sequence considered. A problem we must face is that the calculation of these matrix invariants will become more and more difficult with larger *n* values [17,24,32].

In this paper, based on all of the 2-combinations of the multiset $\{\infty\cdot \mathrm{A}, \infty\cdot \mathrm{G}, \infty\cdot \mathrm{C}, \infty\cdot \mathrm{T}\}$, we propose a novel graphical representation of DNA sequences. Then, according to the idea of "piecewise function", we describe a particular scheme that transforms the graphical representation of DNA into a cell-based descriptor vector. The introduced vector leads to more simple characterizations and comparisons of DNA sequences.

2. Methods

2.1. The 3-D Graphical Representation

As we know, the four nucleic acid bases A, G, C, and T can be classified into three categories:

$$\mathrm{R} = \{\mathrm{A},\mathrm{G}\}/\mathrm{Y} = \{\mathrm{C},\mathrm{T}\};\ \mathrm{M} = \{\mathrm{A},\mathrm{C}\}/\mathrm{K} = \{\mathrm{G},\mathrm{T}\};\ \mathrm{W} = \{\mathrm{A},\mathrm{T}\}/\mathrm{S} = \{\mathrm{G},\mathrm{C}\}.$$

In fact, these groups are just all of the non-repetition 2-combinations of set {A,G,C,T}. If repetition is allowed, in other words, if we consider multiset $\{\infty\cdot \mathrm{A}, \infty\cdot \mathrm{G}, \infty\cdot \mathrm{C}, \infty\cdot \mathrm{T}\}$ instead of the set {A,G,C,T}, then the number of 2-combinations equals 10 (see Table 1).

Table 1. The 2-combinations of multiset $\{\infty\cdot \mathrm{A}, \infty\cdot \mathrm{G}, \infty\cdot \mathrm{C}, \infty\cdot \mathrm{T}\}$.

Base	A	G	C	T
A	{A,A}	{A,G}	{A,C}	{A,T}
G	-	{G,G}	{G,C}	{G,T}
C	-	-	{C,C}	{C,T}
T	-	-	-	{T,T}

Let V be a regular tetrahedron whose center is at the origin $O = (0,0,0)$. V_1 = (+1,+1,+1), V_2 = (−1,−1,+1), V_3 = (+1,−1,−1), and V_4 = (−1,+1,−1) are its four vertices. To each of the vertices we assign one of the four nucleic acid bases A, C, G and T. Moreover, to the midpoint of the line segment AC we assign M, and K to the midpoint of the line segment GT, R to that of the line segment AG, Y to that of the line segment CT, W to that of the line segment AT, and S to that of the line segment CG. We thus obtain ten fixed directions: $\overrightarrow{OA}, \overrightarrow{OC}, \overrightarrow{OG}, \overrightarrow{OT}, \overrightarrow{OM}, \overrightarrow{OK}, \overrightarrow{OR}, \overrightarrow{OY}, \overrightarrow{OW}, \overrightarrow{OS}$, based on which we can derive ten unit vectors:

$$r_A = \frac{1}{||\overrightarrow{OA}||}\cdot\overrightarrow{OA},\ r_C = \frac{1}{||\overrightarrow{OC}||}\cdot\overrightarrow{OC},\ldots,\ r_S = \frac{1}{||\overrightarrow{OS}||}\cdot\overrightarrow{OS} \quad (1)$$

Obviously, the ten unit vectors are ten points on a unit sphere.

An idea arises naturally: each of the ten 2-combinations can be associated with one of the ten unit vectors. In detail, we have

$$\begin{gathered}\{A,A\} \leftarrow r_A,\ \{A,G\} \leftarrow r_R,\ \{A,C\} \leftarrow r_M, \{A,T\} \leftarrow r_W,\\ \{G,G\} \leftarrow r_G, \{G,C\} \leftarrow r_S, \{G,T\} \leftarrow r_K,\\ \{C,C\} \leftarrow r_C,\ \{C,T\} \leftarrow r_Y,\ \{T,T\} \leftarrow r_T.\end{gathered} \tag{2}$$

To obtain the spatial curve of a DNA sequence, we move a unit length in the direction that the above assignment dictates. Taking sequence segment ATGGTGCACCTGACTCCTGATCTGGTA as an example, we inspect it by stepping two nucleotides at a time. Starting from the origin $O = (0,0,0)$, we move in the direction dictated by the first dinucleotide AT, r_W, and arrive at P_1, the first point of the 3-D curve. From this point, we move in the direction dictated by the second dinucleotide TG, r_K, and arrive at the second point P_2. From here we move in the direction dictated by the third dinucleotide GG, r_G, and come to the third point P_3. Continuation of this process is illustrated in Table 2, and the corresponding 3-D graphical representation is shown in Figure 1.

Table 2. Cartesian 3-D coordinates for the sequence ATGGTGCACCTGACTCCTGATCTGGTA.

Point	Dinucleotide	x	y	z
1	AT	0	1	0
2	TG	0	1	−1
3	GG	0.5774	0.4226	−1.5774
4	GT	0.5774	0.4226	−2.5774
5	TG	0.5774	0.4226	−3.5774
6	GC	0.5774	−0.5774	−3.5774
7	CA	0.5774	−0.5774	−2.5774
8	AC	0.5774	−0.5774	−1.5774
9	CC	0	−1.1547	−1
10	CT	−1	−1.1547	−1
...	...	...	...	...

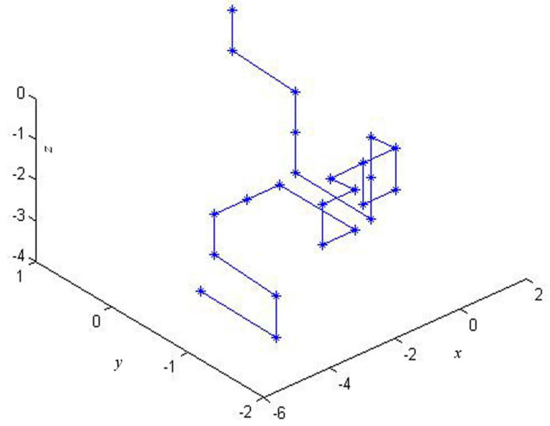

Figure 1. 3-D graphical representation of the sequence ATGGTGCACCTGACTCCTGATCTGGTA.

As the characterization of a research object, a good visualization representation should allow us to see a pattern that may be difficult or impossible to see when the same data is presented in its original form. In order to provide a direct insight into the local and global characteristics of a DNA sequence, the proposed 3-D curve can be projected on planes (x,y), (y,z) or (x,z), and thus three different 2-D graphical representations will be yielded. Figure 2 shows the projections of 3-D curves of 18 different DNA sequences listed in Table 3.

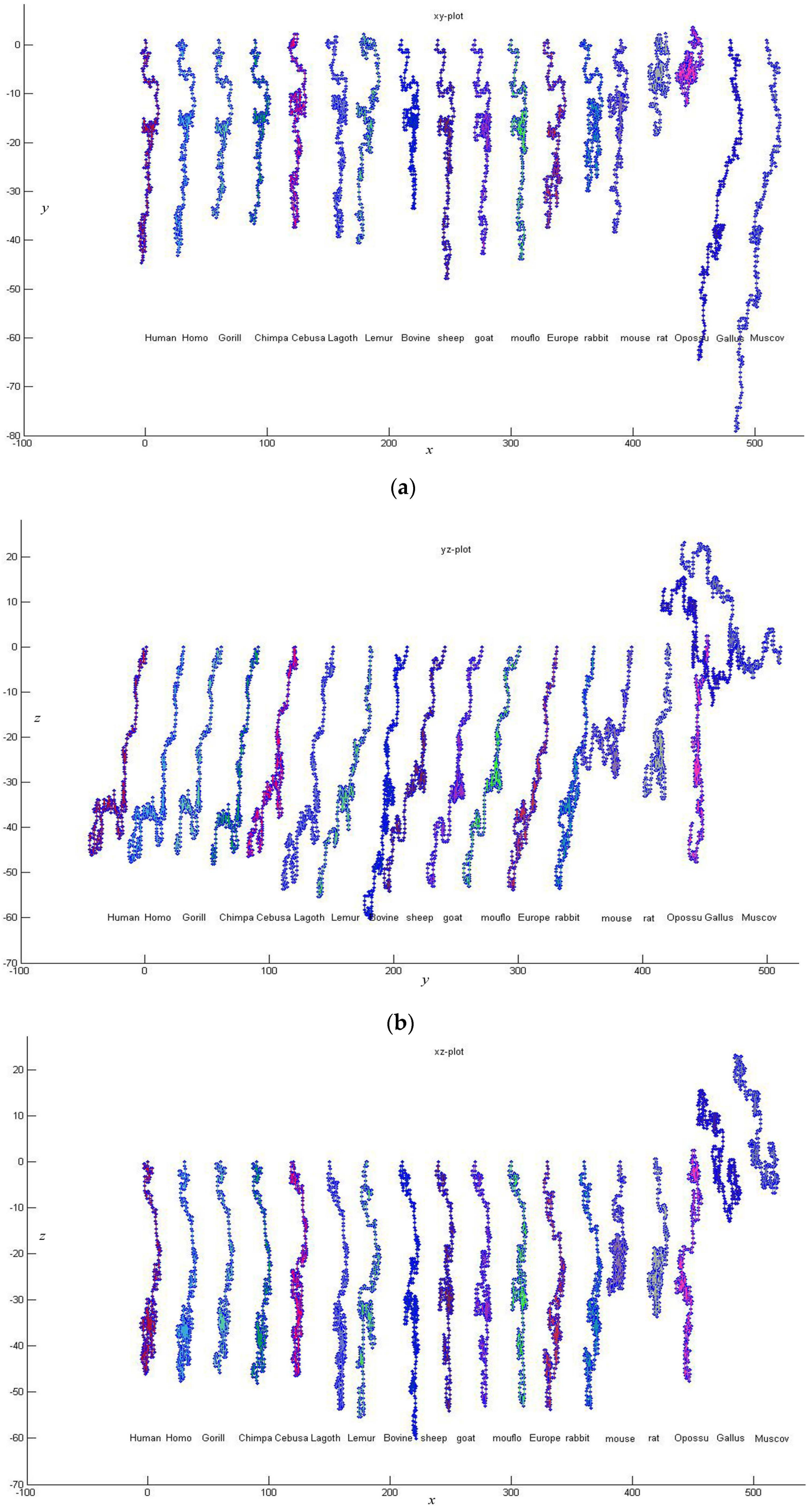

(**a**)

(**b**)

(**c**)

Figure 2. (**a**) The projection on the *xy*-plane of 3-D curves of 18 DNA sequences; (**b**) The projection on the *yz*-plane of 3-D curves of 18 DNA sequences; (**c**) The projection on the *xz*-plane of 3-D curves of 18 DNA sequences.

Table 3. The CDS (Coding DNA Sequence) of β-globin gene of 18 species.

No.	Species	AC (GenBank)	Location
1	*Human*	U01317	join(62187..62278, 62409..62631, 63482..63610)
2	*Homo*	AF007546	join(180..271,402..624,1475..1603)
3	*Gorilla*	X61109	join(4538..4630, 4761..4982, 5833..>5881)
4	*Chimpanzee*	X02345	join(4189..4293, 4412..4633, 5484..>5532)
5	*Lemur*	M15734	join(154..245, 376..598, 1467..1595)
6	*CebusPella*	AY279115	join(946..1037, 1168..1390, 2218..2346)
7	*LagothrixLagotricha*	AY279114	join(952..1043, 1174..1396, 2227..2355)
8	*Bovine*	X00376	join(278..363, 492..714, 1613..1741)
9	*Goat*	M15387	join(279..364, 493..715, 1621..1749)
10	*Sheep*	DQ352470	join(238..323, 452..674, 1580..1708)
11	*Mouflon*	DQ352468	join(238..323, 452..674, 1578..1706)
12	*European hare*	Y00347	join(1485..1576, 1703..1925, 2492..2620)
13	*Rabbit*	V00882	join(277..368, 495..717, 1291..1419)
14	*Mouse*	V00722	join(275..367, 484..705, 1334..1462)
15	*Rat*	X06701	join(310..401, 517..739, 1377..>1505)
16	*Opossum*	J03643	join(467..558, 672..894, 2360..2488)
17	*Gallus*	V00409	join(465..556, 649..871, 1682..1810)
18	*Muscovy duck*	X15739	join(291..382, 495..717, 1742..1870)

It is easy to see that, in each projection, the trend of curves of the two non-mammals (*Gallus*, *Muscovy duck*) is distinguished from that of the mammals. On the other hand, the Primates species are similar to one another, so it is with the curves of *bovine*, *sheep*, *goat*, and *mouflon*. Also, the curves of *rabbit* and *European hare* show their great similarity. In addition, both Figure 2b, the projection on *yz*-plane, and Figure 2c, the projection on *xz*-plane, show *opossum* has relatively low similarity with the remaining mammals, while *mouse* and *rat* look similar to each other because both of their curves wind themselves into a mass and need a relatively small space.

2.2. Numerical Characterization of DNA Sequences

The graphical representations not only offer the visual inspection of data, helping in recognizing major differences among DNA sequences, but also provide with the numerical characterization that facilitates quantitative comparisons of DNA sequences. One way to arrive at the numerical characterization of a DNA sequence is to convert its graphical representation into some structural matrices, and use matrix invariants, e.g., the leading eigenvalues, as descriptors of the DNA sequence [8–18,31,32]. It is expected that effective invariants will emerge and enable to uniquely characterize the sequences considered. However, the difficulties associated with computing various parameters for very large matrices that are natural for long sequences have restricted the numerical characterizations, for instance, leading eigenvalues and the like [17,24]. The search for novel descriptors may be an endless project. The art is in finding useful descriptors, and those that have plausible structural interpretation, at least within the model considered [8]. In this section, we bypass the difficulty of calculating the invariants like the leading eigenvalue and propose a novel descriptor to numerically characterize a DNA sequence.

As described above, the pattern, including shape and trend, of curves for the 18 DNA sequences provides useful information in an efficient way. This inspires us to numerically characterize a DNA sequence with an idea of "piecewise function" as below.

For a given 3-D graphical representation with n vertices, by the order in which these vertices appear in the curve, we partition it into K parts, each of which is called a cell. All the cells contain $m = \left\lfloor \frac{n}{K} \right\rfloor$ vertices except the last one. For the i-th cell, i = 1,2,...,K, the geometric center $U_i = (x_i, y_i, z_i)$ is viewed as its respective. Then we have

$$\overrightarrow{U_{i-1}U_i} = (x_i - x_{i-1}, y_i - y_{i-1}, z_i - z_{i-1}) \tag{3}$$

where $U_0 = (0,0,0)$. It is not difficult to find that $\overrightarrow{U_{i-1}U_i}$ reflects a certain "growing trend" of these cells. For convenience, we call $\overrightarrow{U_{i-1}U_i}$ the trend-point. On the basis of the K trend-points, a DNA sequence can be characterized by a $3K$-dimensional vector V_{tp}:

$$\begin{aligned} V_{tp} = \quad & (x_1 - x_0, x_2 - x_1, \cdots, x_k - x_{k-1}, \\ & y_1 - y_0, y_2 - y_1, \cdots, y_k - y_{k-1}, \\ & z_1 - z_0, z_2 - z_1, \cdots, z_k - z_{k-1}) \end{aligned} \tag{4}$$

In this paper, K is determined by $round\left(\log_4 \frac{\overline{L}}{2\sqrt{2}}\right)$, where $\overline{L} = \frac{1}{N}\sum_{j=1}^{N}\left|s_j\right|$, N is the cardinality of the dataset Ω considered, and $\left|\mathrm{s_j}\right|$ stands for the length of sequence $\mathrm{s_j} \in \Omega$. Taking for example the two non-mammals of the 18 species, the corresponding vectors can be calculated as

$$\begin{aligned} V_{\text{Gallus}} = (&4.524, -9.588, -5.546, -10.962, -9.234, -20.304, \\ &-9.824, -12.093, -4.087, -0.450, 10.255, 5.615), \end{aligned} \tag{5}$$

$$\begin{aligned} V_{\text{MDuck}} = (&6.186, -10.593, -3.440, -12.511, -10.639, -21.519, \\ &-12.987, -18.351, -1.244, 0.498, 10.478, 9.325). \end{aligned} \tag{6}$$

3. Results and Discussion

In this section, we will illustrate the use of the proposed cell-based descriptor V_{tp} of a DNA sequence. For any two sequences S_a and S_b, suppose their descriptor vectors are $a = (a_1, a_2, \cdots, a_{3k})$ and $b = (b_1, b_2, \cdots, b_{3k})$, respectively. Then, their similarity can be examined by the following Euclidean distance. Clearly, the smaller the Euclidean distance is, the more similar the two DNA sequences are.

$$d(a,b) = \sqrt{\sum_{j=1}^{3k}\left(a_j - b_j\right)^2} \tag{7}$$

Firstly, we give a comparison for CDS (Coding DNA Sequence) of β-globin gene of 18 species listed in Table 3. The lengths of the 18 sequences are about 434 bp. Thus K is taken to be 4, and each of these sequences is converted into a 12-D vector. According to Equation (7), we calculate the distance between any two of the 18 DNA sequences. Then an 18 × 18 real symmetric matrix D_{18} is obtained. On the basis of D_{18}, a phylogenetic tree (see Figure 3) is constructed using UPGMA (Unweighted Pair Group Method with Arithmetic Mean) program included in MEGA4 [34]. Observing Figure 3, we find that the CDS are more similar for Primate group {*Gorilla, Chimpanzee, Human, Homo, CebusaPella, LagothrixLagotricha, Lemur*}, Cetartiodactyla group {*bovine, sheep, goat, mouflon*}, Lagomorpha group {*Rabbit, European hare*}, and Rodentia group {*mouse, rat*}, respectively. On the other hand, CDS of the two kinds of non-mammals {*Gallus, Muscovy duck*} are very dissimilar to the mammals because they are grouped into an independent branch. This is analogous to that reported in the literature [8,12,14,31], and the relationship of these species detected by their graphical representations as well. From this result, a conclusion one can draw is that the cell-based descriptors of the new graphical representation may suffice to characterize DNA sequences.

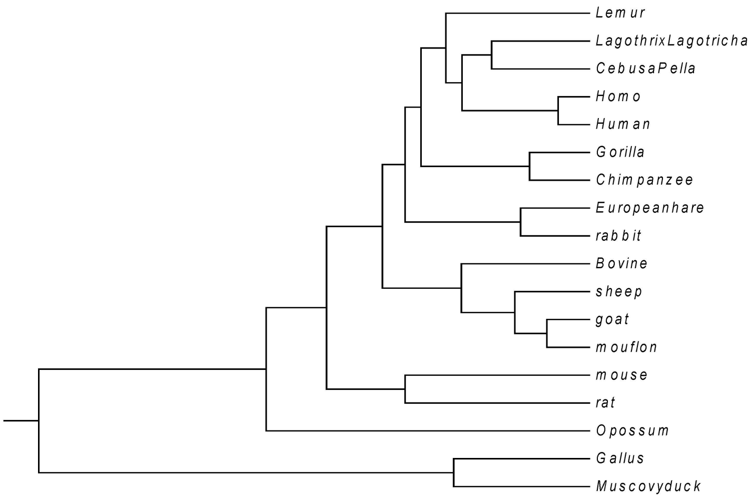

Figure 3. The relationship tree of 18 species.

In order to further illustrate the effectiveness of our method, we test it by phylogenetic analysis on other three datasets: one consists of mitochondrial cytochrome oxidase subunit I (COI) genes of nine butterflies, another includes S segments of 32 hantaviruses (HVs), and the last is composed of 70 complete mitogenomes (mitochondrial genomes). For convenience, we denote the three datasets by COI, HV and mitogenome, respectively. In the COI dataset (see Table 4), which is taken from Yang *et al.* [12], eight belong to the *Catopsilia* genus and one belongs to *Appias* genus, which is used as the out-group. The average length of these COI gene sequences is 661 bp, and thus K, the number of cells, is calculated as 4. According to the method mentioned above, a distance matrix is constructed, and then a phylogenetic tree (see Figure 4) is generated. Figure 4 shows that the five *pomona* sub-species have relatively high similarity with each other, while the two *pyranthe* sub-species cluster together. In addition, *scylla* sub-species is situated at an independent branch, whereas the *Appias lyncida* stays outside of all the *Catopsilia*. This result is consistent with that reported in [12,35].

Table 4. The COI (cytochrome oxidase subunit I) genes of nine butterflies.

NO.	Species	Code	AC (GenBank)	Region
1	*C.pomona pomona f.pomona*	PA	GU446662	Yexianggu, Yunnan
2	*C.pomona pomona f.hilaria*	HI	GU446664	Yexianggu, Yunnan
3	*C.pomona pomona f.crocale*	CR	GU446663	Menglun, Yunnan
4	*C.pomona pomona f.catilla*	CA	GU446666	Daluo, Yunnan
5	*C.pomona pomona f.jugurtha*	JU	GU446665	Daluo, Yunnan
6	*C.scylla scylla*	CS	GU446667	Yinggeling, Hainan
7	*C.pyranthe pyranthe*	CP	GU446668	Daluo, Yunnan
8	*C.pyranthe chryseis*	CH	GU446669	Yinggeling, Hainan
9	*Appias lyncida*	-	GU446670	Bawangling, Hainan

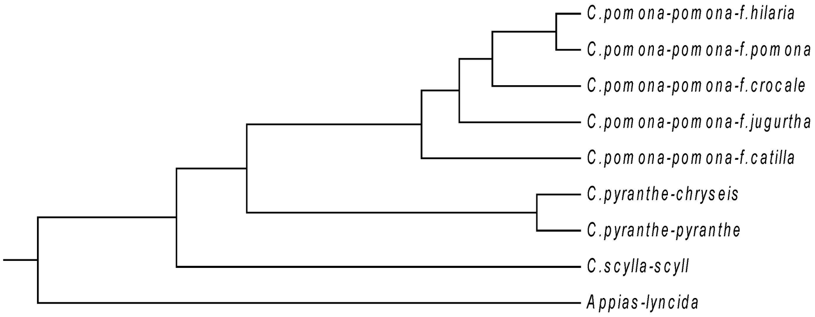
C.pomona-pomona-f.hilaria
C.pomona-pomona-f.pomona
C.pomona-pomona-f.crocale
C.pomona-pomona-f.jugurtha
C.pomona-pomona-f.catilla
C.pyranthe-chryseis
C.pyranthe-pyranthe
C.scylla-scyll
Appias-lyncida

Figure 4. The relationship tree of nine COI (cytochrome oxidase subunit I) gene sequences.

The hantavirus (HV), which is named for the Hantan River area in South Korea, is a relatively newly discovered RNA virus in the family *Bunyaviridae*. This kind of virus normally infects rodents and does not cause disease in these hosts. Humans may be infected with HV, and some HV strains could cause severe, sometimes fatal, diseases in humans, such as HFRS (hantavirus hemorrhagic fever with renal syndrome) and HPS (hantavirus pulmonary syndrome). The later occurred in North and South America, while the former mainly in Eurasia [12,36]. In Eastern Asia, particularly in China and Korea, the viruses that cause HFRS mainly include Hantaan (HTN) and Seoul (SEO) viruses, while Puumala (PUU) virus is found in Western Europe, Russia and northeastern China. The HV dataset analyzed in this paper includes 32 HV sequences. Phlebovirus (PV) is another genus of the family *Bunyaviridae*. Here, two PV strains KF297911 and KF297914 are used as the out-group. The name, accession number, type, and region of the 34 sequences are described in Table 5. The lengths of these sequences are in the range of 1.30–1.88 kbp. Thus K is calculated as 5, and each of the 34 viruses is converted into a 15-D vector. The phylogenetic tree constructed by our method is shown in Figure 5.

Table 5. Sequence information of S segment of hantavirus.

No.	Strain	AC (GenBank)	Type	Region
1	CGRn53	EF990907	HTNV	Guizhou
2	CGRn5310	EF990906	HTNV	Guizhou
3	CGRn93MP8	EF990905	HTNV	Guizhou
4	CGRn8316	EF990903	HTNV	Guizhou
5	CGRn9415	EF990902	HTNV	Guizhou
6	CGRn93P8	EF990904	HTNV	Guizhou
7	CGHu3612	EF990909	HTNV	Guizhou
8	CGHu3614	EF990908	HTNV	Guizhou
9	Z10	AF184987	HTNV	Shengzhou
10	Z5	EF103195	HTNV	Shengzhou
11	NC167	AB027523	HTNV	Anhui
12	CGAa4MP9	EF990915	HTNV	Guizhou
13	CGAa4P15	EF990914	HTNV	Guizhou
14	CGAa1011	EF990913	HTNV	Guizhou
15	CGAa1015	EF990912	HTNV	Guizhou
16	H5	AB127996	HTNV	Heilongjiang
17	76-118	M14626	HTNV	South Korea
18	Gou3	AF184988	SEOV	Jiande
19	ZJ5	FJ753400	SEOV	Jiande
20	80-39	AY273791	SEOV	South Korea
21	SR11	M34881	SEOV	Japan
22	K24-e7	AF288653	SEOV	Xinchang
23	K24-v2	AF288655	SEOV	Xinchang
24	Z37	AF187082	SEOV	Wenzhou
25	ZT10	AY766368	SEOV	Tiantai
26	ZT71	AY750171	SEOV	Tiantai
27	K27	L08804	PUUV	Russia
28	P360	L11347	PUUV	Russia
29	Sotkamo	X61035	PUUV	Finland
30	Fusong843-06	EF488805	PUUV	Jilin
31	Fusong199-05	EF488803	PUUV	Jilin
32	Fusong900-06	EF488806	PUUV	Jilin
33	91045-AG	KF297911	PV	Iran
34	I-58	KF297914	PV	Iran

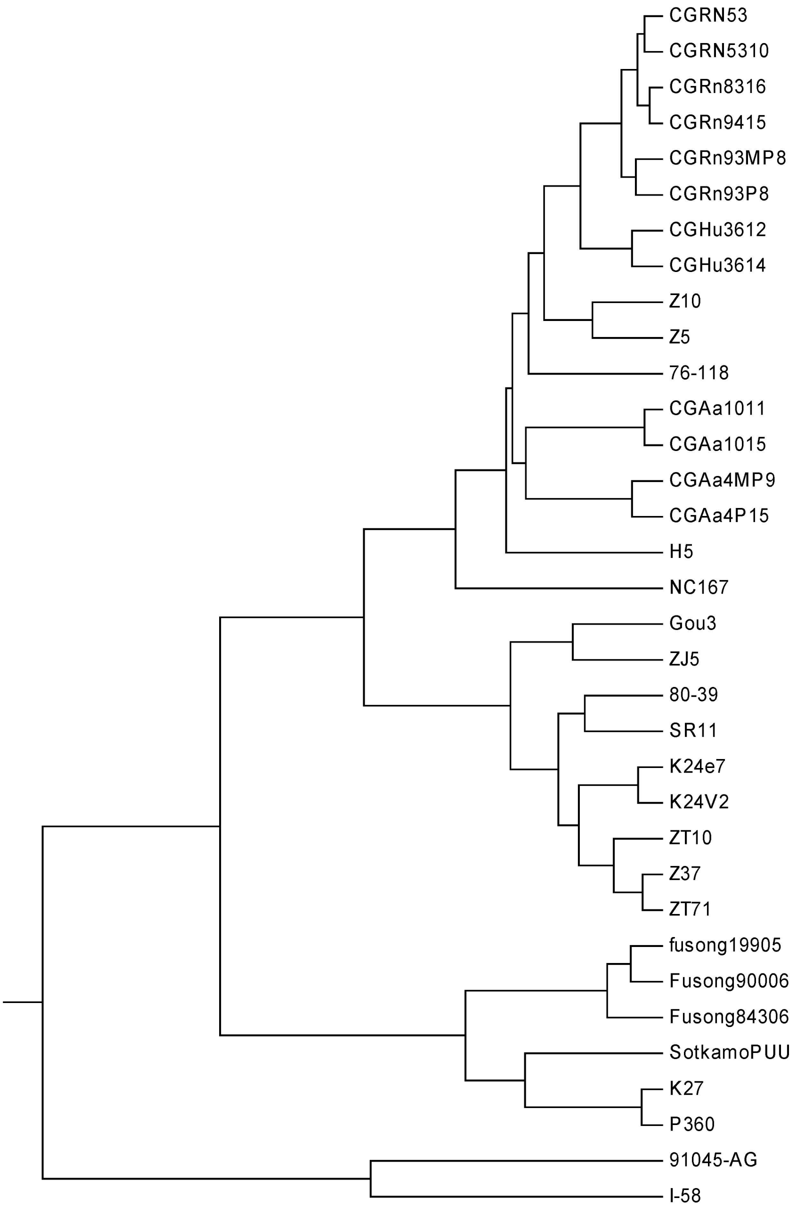

Figure 5. The relationship tree of 34 viruses.

From Figure 5, we find that the two PV strains form an independent branch, which can be distinguished easily from the HV strains, while the 32 HVs are grouped into three separate branches: the strains belonging to PUUV are clearly clustered together, the strains belonging to SEOV appear to cluster together, and so do the ones belonging to HTNV. A closer look at the subtree of HTNV, all CGRn strains whose host is *Rattus norvegicus* tend to cluster together, so it is with the CGHu strains whose host is Homo sapiens. In addition, all the four CGAa strains whose host is *Apodemus agrarius* are grouped closely. Needless to say, the phylogeny is not only closely related to the isolated regions, but also has certain relationship with the host. This result is similar to that reported in [12,37].

The mitogenome dataset comprises 70 complete mitochondrial genomes of Eukaryota. The name, accession number, and genome length are listed in Table 6. Among them, two species (*Argopecten irradians irradians* and *Argopecten purpuratus*) belong to family Pectinidae are used as the out-group. Four species belong to the Order Caudata under the Class Amphibia, while four species belong to the Order Anura under the same Class. The remaining belongs to the Class Actinopterygii. The average length of the 70 genome sequences is about 16817 bp. Thus, *K* is calculated as 6, and each of these genome sequences is converted into an 18-D vector. The phylogenetic tree constructed by our method is shown in Figure 6. It is easy to see from Figure 6 that the two *Pectinidae* species stay outside of the others, while the four *Hynobiidae* species and four *Ranidae* species form an independent branch. In the subtree of the Class Actinopterygii, the 60 genomes are separated into six groups: group 1 corresponds to genus *Anguilla* under family Anguillidae; group 2 includes genera *Bangana* and *Acrossocheilus* under family Cyprinidae; group 3 includes genera *Brachymystax* and *Hucho* under family Salmonidae; group 4 is genus *Alepocephalus* under family Alepocephalidae; group 5 is the family of Clupeidae; group 6 includes genera *Trichiurus*, *Amphiprion* and *Apolemichthys* under Acanthomorphata. This result agrees well with the established taxonomic groups. In addition, we make a comparison for the 70 genome sequences by using ClustalX2.1 [38], and the corresponding tree is shown in Figure 7. Observing Figure 7, we find that the tree includes four branches: the outside is the *Argopecten* branch, the following is *Babina*, then *Batrachuperus*, and the subtree consisting of the other 60 species. A closer look at the subtree shows that *Trichiurus* is distinguished from the remaining, which seems to be a disappointing phenomenon in the evolutionary sense.

Table 6. Sequence information of 70 complete mitogenomes.

No.	Genome	AC (GenBank)	Length
1	*Acrossocheilus barbodon*	NC_022184	16596
2	*Acrossocheilus beijiangensis*	NC_028206	16600
3	*Acrossocheilus fasciatus*	NC_023378	16589
4	*Acrossocheilus hemispinus*	NC_022183	16590
5	*Acrossocheilus kreyenbergii*	NC_024844	16849
6	*Acrossocheilus monticola*	NC_022145	16599
7	*Acrossocheilus parallens*	NC_026973	16592
8	*Acrossocheilus stenotaeniatus*	NC_024934	16594
9	*Acrossocheilus wenchowensis*	NC_020145	16591
10	*Alepocephalus agassizii*	NC_013564	16657
11	*Alepocephalus australis*	NC_013566	16640
12	*Alepocephalus bairdii*	NC_013567	16637
13	*Alepocephalus bicolor*	NC_011012	16829
14	*Alepocephalus productus*	NC_013570	16636
15	*Alepocephalus tenebrosus*	NC_004590	16644
16	*Alepocephalus umbriceps*	NC_013572	16640
17	*Alosa alabamae*	NC_028275	16708
18	*Alosa alosa*	NC_009575	16698
19	*Alosa pseudoharengus*	NC_009576	16646
20	*Alosa sapidissima*	NC_014690	16697
21	*Amphiprion bicinctus*	NC_016701	16645
22	*Amphiprion clarkia*	NC_023967	16976
23	*Amphiprion frenatus*	NC_024840	16774
24	*Amphiprion ocellaris*	NC_009065	16649
25	*Amphiprion percula*	NC_023966	16645
26	*Amphiprion perideraion*	NC_024841	16579
27	*Amphiprion polymnus*	NC_023826	16804
28	*Anguilla anguilla*	NC_006531	16683
29	*Anguilla australis*	NC_006532	16686
30	*Anguilla australis schmidti*	NC_006533	16682
31	*Anguilla bengalensis labiata*	NC_006543	16833
32	*Anguilla bicolor bicolor*	NC_006534	16700
33	*Anguilla bicolor pacifica*	NC_006535	16693
34	*Anguilla celebesensis*	NC_006537	16700
35	*Anguilla dieffenbachia*	NC_006538	16687
36	*Anguilla interioris*	NC_006539	16713
37	*Anguilla japonica*	NC_002707	16685
38	*Anguilla luzonensis* (Philippine eel)	NC_011575	16635

Table 6. *Cont.*

No.	Genome	AC (GenBank)	Length
39	*Anguilla luzonensis* (freshwater eel)	NC_013435	16632
40	*Anguilla malgumora*	NC_006536	16550
41	*Anguilla marmorata*	NC_006540	16745
42	*Anguilla megastoma*	NC_006541	16714
43	*Anguilla mossambica*	NC_006542	16694
44	*Anguilla nebulosa nebulosa*	NC_006544	16707
45	*Anguilla obscura*	NC_006545	16704
46	*Anguilla reinhardtii*	NC_006546	16690
47	*Anguilla rostrata*	NC_006547	16678
48	*Apolemichthys armitagei*	NC_027857	16551
49	*Apolemichthys griffisi*	NC_027592	16528
50	*Apolemichthys kingi*	NC_026520	16816
51	*Argopecten irradians irradians*	NC_012977	16211
52	*Argopecten purpuratus*	NC_027943	16270
53	*Babina adenopleura*	NC_018771	18982
54	*Babina holsti*	NC_022870	19113
55	*Babina okinavana*	NC_022872	19959
56	*Babina subaspera*	NC_022871	18525
57	*Bangana decora*	NC_026221	16607
58	*Bangana tungting*	NC_027069	16543
59	*Batrachuperus londongensis*	NC_008077	16379
60	*Batrachuperus pinchonii*	NC_008083	16390
61	*Batrachuperus tibetanus*	NC_008085	16379
62	*Batrachuperus yenyuanensis*	NC_012430	16394
63	*Brachymystax lenok*	NC_018341	16832
64	*Brachymystax lenok tsinlingensis*	NC_018342	16669
65	*Brachymystax tumensis*	NC_024674	16836
66	*Hucho bleekeri*	NC_015995	16997
67	*Hucho hucho*	NC_025589	16751
68	*Hucho taimen*	NC_016426	16833
69	*Trichiurus lepturus nanhaiensis*	NC_018791	17060
70	*Trichiurus japonicus*	NC_011719	16796

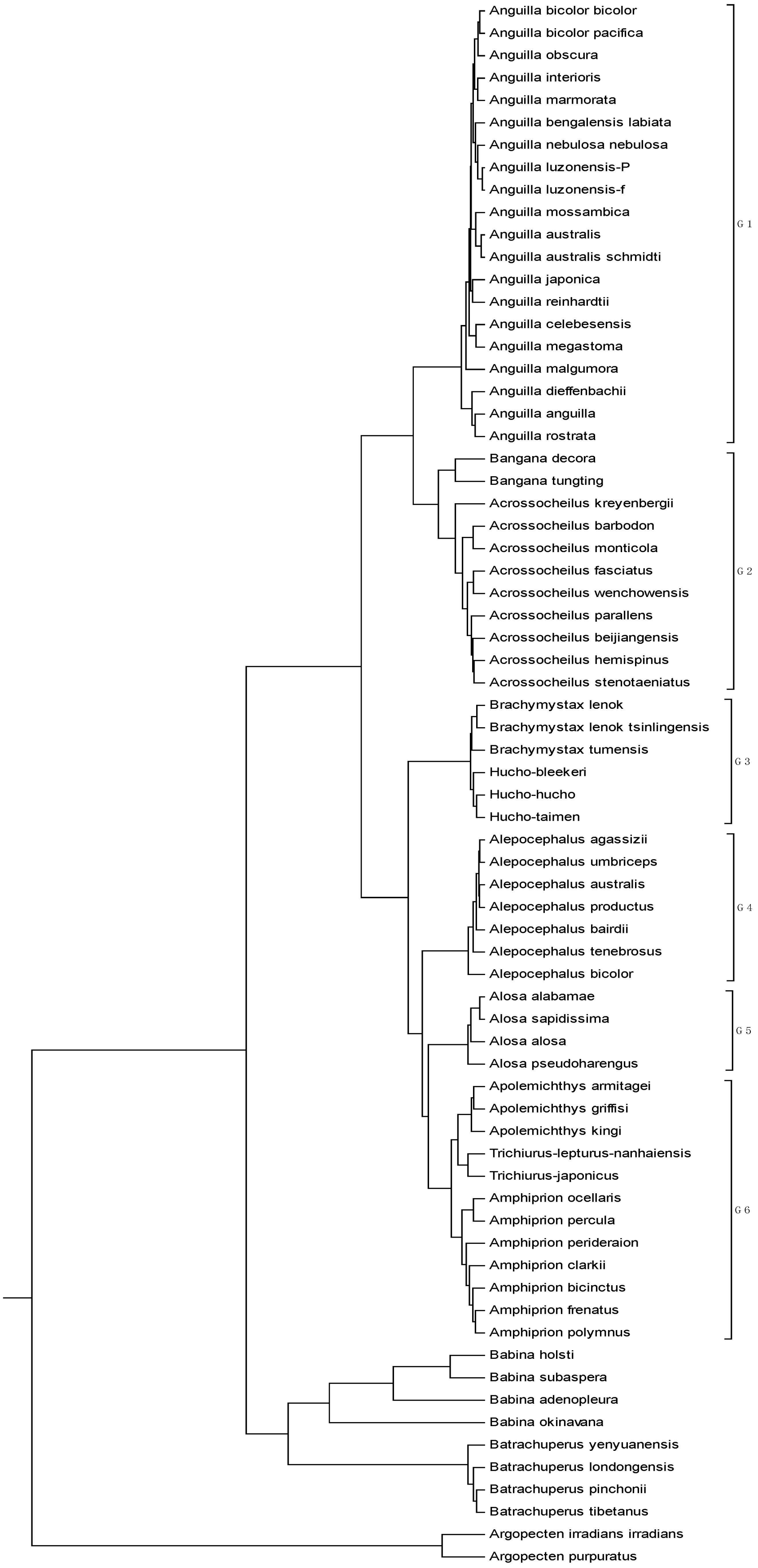

Figure 6. The tree of 70 genome sequences constructed with the current method.

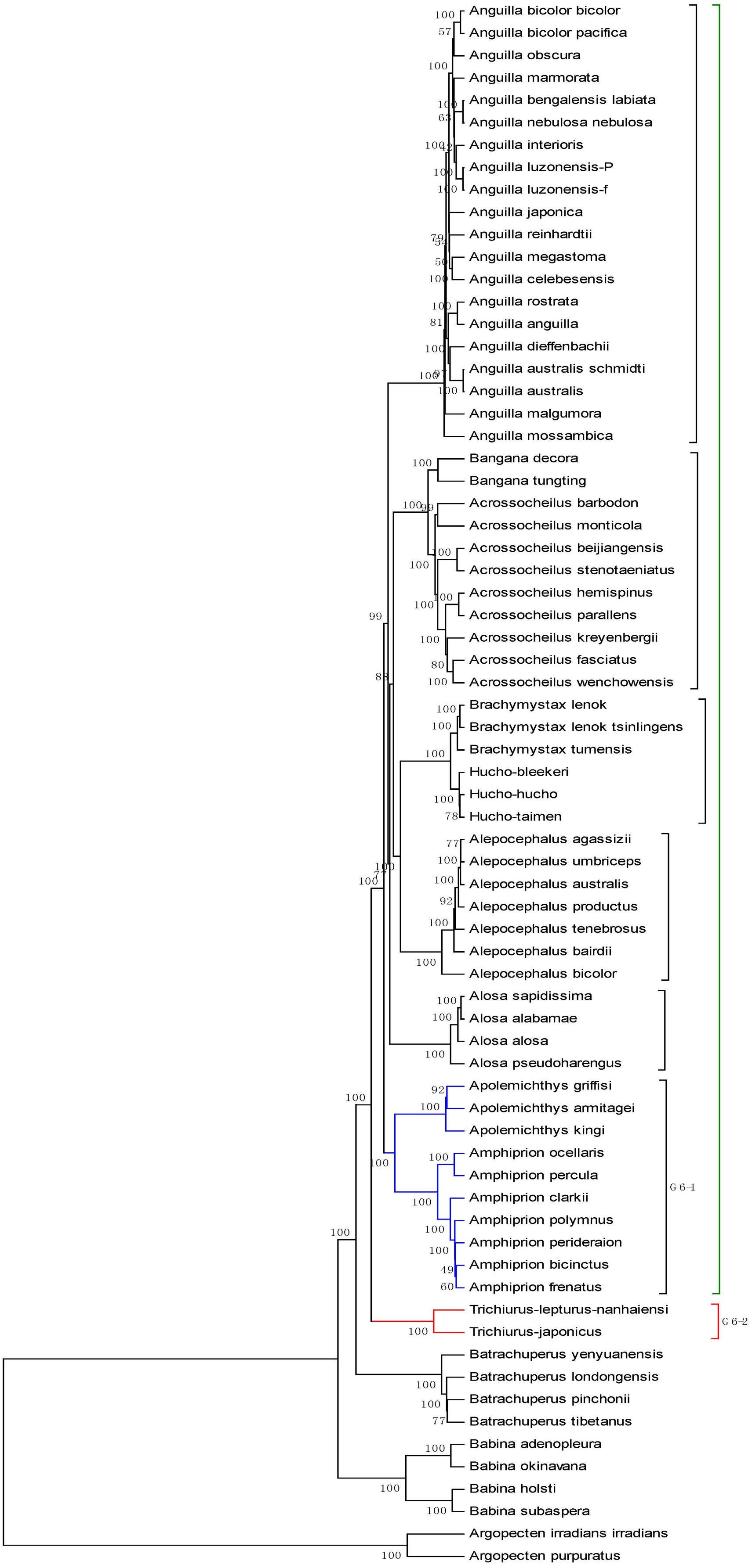

Figure 7. The tree of 70 genome sequences constructed with multiple alignment.

4. Concluding Remarks

By means of a regular tetrahedron whose center is at the origin, we associate the ten 2-combinations of multiset $\{\infty \cdot A, \infty \cdot G, \infty \cdot C, \infty \cdot T\}$ with ten unit vectors (points on a unit sphere), and then a novel 3-D graphical representation of a DNA sequence is proposed. Moreover, we partition the graph into K cells, and then a $3K$-dimensional cell-based vector is used to numerically characterize a DNA sequence. The proposed method is tested by phylogenetic analysis on four datasets. In comparison with other methods, our approach does not depend on multiple sequence alignment, and avoids the complex calculation as in the calculation of invariants for higher order matrices. Nevertheless, K, the number of cells, is dataset specific, which may restrict our approach. We will make efforts in our future work to find a possible formula for K that is independent of the dataset.

Acknowledgments: The authors wish to thank the three anonymous referees for their valuable suggestions and support. This work was partially supported by the National Natural Science Foundation of China (No. 11171042), the Program for Liaoning Innovative Research Team in University (LT2014024), the Liaoning BaiQianWan Talents Program (2012921060), and the Open Project Program of Food Safety Key Lab of Liaoning Province (LNSAKF2011034).

Author Contributions: Chun Li and Xiaoqing Yu conceived the study and drafted the manuscript. Wenchao Fei and Yan Zhao participated in the design of the study and analysis of the results.

Conflicts of Interest: The authors declare no conflict of interest.

References

1. Tian, K.; Yang, X.Q.; Kong, Q.; Yin, C.C.; He, R.L.; Yau, S.S.T. Two dimensional Yau-hausdorff distance with applications on comparison of DNA and protein sequences. *PLoS ONE* **2015**, *10*. [CrossRef] [PubMed]
2. Hamori, E.; Ruskin, J. H curves, a novel method of representation of nucleotide series especially suited for long DNA sequences. *J. Biol. Chem.* **1983**, *258*, 1318–1327. [PubMed]
3. Gates, M.A. Simpler DNA sequence representations. *Nature* **1985**, *316*. [CrossRef]
4. Nandy, A. A new graphical representation and analysis of DNA sequence structure: I methodology and application to globin genes. *Curr. Sci.* **1994**, *66*, 309–314.
5. Nandy, A. Graphical representation of long DNA sequences. *Curr. Sci.* **1994**, *66*, 821.
6. Leong, P.M.; Morgenthaler, S. Random walk and gap plots of DNA sequences. *Comput. Appl. Biosci.* **1995**, *11*, 503–507. [CrossRef] [PubMed]
7. Jeffrey, H.J. Chaos game representation of gene structure. *Nucleic Acids Res.* **1990**, *18*, 2163–2170. [CrossRef] [PubMed]
8. Randic, M.; Vracko, M.; Nandy, A.; Basak, S.C. On 3-D graphical representation of DNA primary sequences and their numerical characterization. *J. Chem. Inf. Comput. Sci.* **2000**, *40*, 1235–1244. [CrossRef] [PubMed]
9. Randic, M.; Novic, M.; Plavsic, D. Milestones in graphical bioinformatics. *Int. J. Quantum Chem.* **2013**, *113*, 2413–2446. [CrossRef]
10. Randic, M.; Zupan, J.; Balaban, A.T.; Vikic-Topic, D.; Plavsic, D. Graphical representation of proteins. *Chem. Rev.* **2011**, *111*, 790–862. [CrossRef] [PubMed]
11. Li, C.; Tang, N.N.; Wang, J. Directed graphs of DNA sequences and their numerical characterization. *J. Theor. Biol.* **2006**, *241*, 173–177. [CrossRef] [PubMed]
12. Yang, Y.; Zhang, Y.Y.; Jia, M.D.; Li, C.; Meng, L.Y. Non-degenerate graphical representation of DNA sequences and its applications to phylogenetic analysis. *Comb. Chem. High Throughput Screen.* **2013**, *16*, 585–589. [CrossRef] [PubMed]
13. Gonzzlez-Diaz, H.; Perez-Montoto, L.G.; Duardo-Sanchez, A.; Paniagua, E.; Vazquez-Prieto, S.; Vilas, R.; Dea-Ayuela, M.A.; Bolas-Fernandez, F.; Munteanu, C.R.; Dorado, J.; *et al.* Generalized lattice graphs for 2D-visualization of biological information. *J. Theor. Biol.* **2009**, *261*, 136–147. [CrossRef] [PubMed]
14. Zhang, Z.J. DV-Curve: A novel intuitive tool for visualizing and analyzing DNA sequences. *Bioinformatics* **2009**, *25*, 1112–1117. [CrossRef] [PubMed]
15. Qi, Z.H.; Jin, M.Z.; Li, S.L.; Feng, J. A protein mapping method based on physicochemical properties and dimension reduction. *Comput. Biol. Med.* **2015**, *57*, 1–7. [CrossRef] [PubMed]

16. Waz, P.; Bielinska-Waz, D. 3D-dynamic representation of DNA sequences. *J. Mol. Model.* **2014**, *20*. [CrossRef] [PubMed]
17. Yao, Y.H.; Yan, S.; Han, J.; Dai, Q.; He, P.A. A novel descriptor of protein sequences and its application. *J. Theor. Biol.* **2014**, *347*, 109–117. [CrossRef] [PubMed]
18. Ma, T.T.; Liu, Y.X.; Dai, Q.; Yao, Y.H.; He, P.A. A graphical representation of protein based on a novel iterated function system. *Phys. A* **2014**, *403*, 21–28. [CrossRef]
19. Zhang, R.; Zhang, C.T. A brief review: The Z curve theory and its application in genome analysis. *Curr. Genom.* **2014**, *15*, 78–94. [CrossRef] [PubMed]
20. Zhang, C.T.; Zhang, R.; Ou, H.Y. The Z curve database: A graphic representation of genome sequences. *Bioinformatics* **2003**, *19*, 593–599. [CrossRef] [PubMed]
21. Zhang, R.; Zhang, C.T. Z curves, an intuitive tool for visualizing and analyzing DNA sequences. *J. Biomol. Struct. Dyn.* **1994**, *11*, 767–782. [CrossRef] [PubMed]
22. Herisson, J.; Payen, G.; Gherbi, R. A 3D pattern matching algorithm for DNA sequences. *Bioinformatics* **2007**, *23*, 680–686. [CrossRef] [PubMed]
23. Bianciardi, G.; Borruso, L. Nonlinear analysis of tRNAs squences by random walks: Randomness and order in the primitive information polymers. *J. Mol. Evol.* **2015**, *80*, 81–85. [CrossRef] [PubMed]
24. Ghosh, A.; Nandy, A. Graphical representation and mathematical characterization of protein sequences and applications to viral proteins. *Adv. Protein Chem. Struct. Biol.* **2011**, *83*. [CrossRef]
25. Karlin, S.; Burge, C. Dinucleotide relative abundance extremes: A genomic signature. *Trends Genet.* **1995**, *11*, 283–290. [PubMed]
26. Karlin, S. Global dinucleotide signatures and analysis of genomic heterogeneity. *Curr. Opin. Microbiol.* **1998**, *1*, 598–610. [CrossRef]
27. Yang, X.W.; Wang, T.M. Linear regression model of short *k*-word: A similarity distance suitable for biological sequences with various lengths. *J. Theor. Biol.* **2013**, *337*, 61–70. [CrossRef] [PubMed]
28. Li, C.; Ma, H.; Zhou, Y.; Wang, X.; Zheng, X. Similarity analysis of DNA sequences based on the weighted pseudo-entropy. *J. Comput. Chem.* **2011**, *32*, 675–680. [CrossRef] [PubMed]
29. Rocha, E.P.; Viari, A.; Danchin, A. Oligonucleotide bias in *Bacillus subtilis*: General trends and taxonomic comparisons. *Nucleic Acids Res.* **1998**, *26*, 2971–2980. [CrossRef] [PubMed]
30. Pride, D.T.; Meineramann, R.J.; Wassenaar, T.M.; Blaser, M.J. Evolutionary implications of microbial genome tetranucleotide frequency biases. *Genome Res.* **2003**, *13*, 145–158. [CrossRef] [PubMed]
31. Li, C.; Wang, J. Numerical characterization and similarity analysis of DNA sequences based on 2-D graphical representation of the characteristic sequences. *Comb. Chem. High. Throughput Screen.* **2003**, *6*, 795–799. [CrossRef] [PubMed]
32. Li, C.; Wang, J. New invariant of DNA sequences. *J. Chem. Inf. Model.* **2005**, *36*, 115–120. [CrossRef] [PubMed]
33. Bai, F.; Zhang, J.; Zheng, J.; Li, C.; Liu, L. Vector representation and its application of DNA sequences based on nucleotide triplet codons. *J. Mol. Graph. Model.* **2015**, *62*, 150–156. [CrossRef] [PubMed]
34. MEGA, Molecular Evolutionary Genetics Analysis. Available online: http://www.megasoftware.net (accessed on 15 January 2014).
35. Wang, J.; Shang, S.Q.; Zhang, Y.L. Phylogenetic relationship of genus catopsilia (Lepidoptera: Pieridae) based on partial sequences of NDI and COI genes from China. *Acta. Zootaxon. Sin.* **2010**, *35*, 776–781.
36. Zhang, Y.Z.; Dong, X.; Li, X.; Ma, C.; Xiong, H.P.; Yan, G.J.; Gao, N.; Jiang, D.M.; Li, M.H.; Li, L.P.; *et al*. Seoul virus and hantavirus disease, Shenyang, People's Republic of China. *Emerg. Infect. Dis.* **2009**, *15*, 200–206. [CrossRef] [PubMed]
37. Yao, P.P.; Zhu, H.P.; Deng, X.Z.; Xu, F.; Xie, R.H.; Yao, C.H.; Weng, J.Q.; Zhang, Y.; Yang, Z.Q.; Zhu, Z.Y. Molecular evolution analysis of hantaviruses in Zhejiang province. *Chin. J. Virol.* **2010**, *26*, 465–470.
38. Clustal: Multiple Sequence Alignment. Available online: http://www.clustal.org (accessed on 31 August 2012).